Modeling results on detectability of shallow tunnels using Rayleigh-wave diffraction

Chong Zeng, Jianghai Xia and Richard D. Miller, Kansas Geological Survey, The University of Kansas, Georgios P. Tsoflias, Department of Geology, The University of Kansas*

Summary

Rayleigh waves have been widely employed in near-surface high-resolution seismic investigations since the development of multi-channel analysis of surface waves (MASW). Usually, detecting near-surface features such as voids and tunnels by inverting Rayleigh-wave phase velocities is challenging because the resolution of inverted shear (S)-wave velocity profiles is limited by a geophone-spread length. As a human-made structure, a shallow tunnel can generate strong diffractions of seismic waves due to its angular shape and the high contrast elastic modulus around a tunnel surface. Since Rayleigh-wave energy is dominant in the near-surface P-SV wavefield, the diffraction of Rayleigh waves is also significant on a shotgather, which allows a tunnel to be located directly by using a hyperbola curve matching technique. However, the size and depth of the tunnel can influence the diffraction energy dramatically. In case where the diffraction energy is too weak, it is usually impractical to recognize the hyperbolic pattern on a shotgather even with F-K filtering. In this paper, we present finite-difference numerical modeling results illustrating the variation of Rayleigh-wave diffraction energy for different size tunnels. The modeling results reveal that the amplitude of Rayleigh-wave diffraction decreases at different rate depending on tunnel size The diffraction energy decreases more rapidly when the size of a tunnel is smaller than 3/16 of the central depth of the tunnel. When a tunnel size is smaller than 1/32 of its depth, the diffraction energy of Rayleigh-wave is less than 1% of the direct Rayleigh-wave energy, which makes the hyperbola difficult to be recognized on a shotgather. Considering the noise and near-surface attenuation in a real data, the ratio of size to depth of a detectable tunnel could be much larger than these modeling based results.

Introduction

Since the development of MASW technique (e.g., Song et al. 1989), surface-wave methods have been widely used in near-surface high-resolution seismic surveys. By inverting Rayleigh-wave phase velocities (Xia et al., 1999), a reliable S-wave velocity profile can be generated with errors no more than 15% (Xia et al., 1999; Xia et al., 2002). The surface-wave methods have been applied successfully in various near-surface seismic investigations (e.g., Miller et al., 1999; Xia et al., 2004). However, it is not suitable to investigate near-surface features such as tunnels, voids and faults (Xia et al., 2005; Xia et al., 2007). This is mainly because the MASW based surface-wave methods only consider layered earth models. Although some special non-layered earth model can be used (Xia et al., 2006), generating S-wave velocity profiles for most 2-D structures is still challenging. The resolution limitations of the inverted S-wave velocity profile make it difficult to directly apply it to tunnel detection.

Shallow tunnels are often human-made and angular. They are usually relatively small and filled with air. The wall of a tunnel can be considered as a high contrast interface during the propagation of seismic waves. According to Huygens–Fresnel principle, diffraction can occur when seismic waves encounter the corner of a tunnel. Rayleigh-wave energy is dominant in a near-surface P-SV wavefield and the diffraction of Rayleigh waves can be significant. This makes Rayleigh-wave diffraction easily recognizable on a shotgather. Campman et al. (2004) studied surface-wave scattering from voids. Xia et al. (2007) demonstrated that it is feasible to use Rayleigh-wave diffraction to detect near-surface 2-D structures such as voids, faults and tunnels. They developed a simple method in time-space domain to detect near-surface features based a travel time equation of surface-wave diffractions. After F-K filtering, the direct arrived Rayleigh waves are filtered so that the diffraction energy of the Rayleigh waves can be enhanced. Then a tunnel can be easily located using a hyperbola curve matching technique.

The diffraction energy of Rayleigh waves can be influenced by various factors. Based on the modeling studies of Gelis et al. (2005), shallower cavities generate stronger diffraction energy. For cavities at a same depth, an angular void generates more severe perturbations than a circular feature. Low velocity zones around and above a cavity can enhance the diffraction energy. For tunnel detection using Rayleigh-wave diffraction, the most important step is to recognize the hyperbola of diffraction pattern on a shotgather. Hence the diffraction energy is key to the detectability of a tunnel. Although the diffraction amplitude can be enhanced by F-K filtering, it is often superimposed with noise (e.g. converted waves, air-coupled waves) in real data. In the case where the diffraction energy is too weak, even filtering cannot discriminate it from noise. In this paper, we discuss the relationships between the diffraction energy and the ratio of size to depth of a tunnel through finite-difference modeling. We also estimate the minimum detectability size of tunnel if the depth known. During the modeling, the only attenuation of energy is caused by spherical divergence. For real data, this ratio should be larger due to the presence of noise and near-surface signal attenuation.

Rayleigh-wave diffraction

As surface waves propagate along the ground surface with a dominant phase velocity, diffraction of Rayleigh waves can occur at a corner of a tunnel, which will generate hyperbolic patterns on a shotgather. The following travel time equation was derived by Xia et al. (2007):

$$t_x = \frac{1}{v}\left(d + \sqrt{x^2 + h^2}\right), \qquad (1)$$

where t_x is the arrival time of the diffracted Rayleigh waves, x is the horizontal distance between a receiver and the corner of a tunnel (the diffractor), v is the dominant phase velocity of the diffraction, d is the horizontal distance between the source and the diffractor, h is the depth of a tunnel. With this equation, the horizontal location and the depth of a tunnel can be easily determined based on travel time data from a diffraction curve.

In a homogenous half-space, The Rayleigh-wave phase velocity is a constant. So the diffracted wave velocity is also a constant, which is the v in equation (1). In case where the tunnel lies in a heterogeneous medium, for example, a layered earth model, the diffracted wave velocity could be considered as an averaged phase velocity (Xia et al., 2007). In theory, diffraction occurs at each corner of the tunnel. However, for relatively small shallow tunnels, the diffractions generated by each corner will superimposed together and are not easy to differentiate. So the tunnel can be considered as a point anomaly that radiates the diffraction energy from the center of the tunnel. In this case, the depth of the tunnel [h in equation (1)] is the central point location rather than the top depth of a tunnel surface.

Directly arrived Rayleigh-wave attenuates less than P-waves along the ground surface. However, the energy of Rayleigh-waves attenuates exponentially with increasing depth. This is also true for diffracted Rayleigh waves. Gelis et al. (2005) showed that the diffraction energy of Rayleigh waves changes dramatically with the variation of depth of cavities. A void strongly affects the seismograms when it is near to the ground surface. To detect a deeper tunnel, the source must generate lower frequency surface waves. This usually causes more complicated interference of the surface waves and converted waves, thus, makes it more difficult to recognize Rayleigh-wave diffraction. Although F-K filtering can enhance the energy of Rayleigh-wave diffraction, it is still challenging to separate surface-wave diffraction and converted waves on the seismogram. When the tunnel is deep enough, or the tunnel size is too small, the diffraction energy of Rayleigh waves is usually too weak to be differentiated from the background noise because the complexity of near-surface materials.

Modeling of surface-wave diffraction

Since no explicit attenuation (e.g., the near-surface attenuation) was accounted for in our modeling process, the only energy attenuation of seismic waves is caused by spherical divergence. In 2-D modeling, the energy of seismic waves decay with distance as circular wavefronts spread out. For a single trace recorded at a same location for different models, amplitudes of seismic waves are directly comparable due to the same energy attenuation. Hence, for this case, Rayleigh-wave diffraction energy can be analyzed quantitatively by comparing the absolute values of the vertical particle velocities on a single trace record.

We made a set of 2-D models to estimate the variation of Rayleigh-wave diffraction energy. All the models are exactly the same except for the size of the tunnel. For simplicity, we use the 2-D model of a tunnel located in a homogeneous half-space. The tunnel is described by a square filled with air. In horizontal direction, the tunnel is located at the center of the receiver array. The central depth of the tunnel is 8 m. The size of the modeled tunnel varies from 4 m to 0.125 m. The horizontal distance between the source and the center of the tunnel is 30 m. The horizontal coordinate of the source is 0 m. Sixty synthetic receivers are distributed from 1 m to 60 m equidistantly with 1 m interval. The source and all the receivers are located on the free surface.

To generate strong Rayleigh-wave motion, we use a vertical point source. The source wavelet is a Ricker wavelet whose central frequency is 23.8 Hz with 50 ms delay in time domain. The P-wave velocity in the homogeneous part of the model is 800 m/s, the S-wave velocity is 200 m/s, and the density is 2.0 g/cm^3. According to the analytical solution of Lamb's problem, we know that the Rayleigh-wave phase velocity in this homogeneous half-space is 190.225 m/s. Hence, the dominant wavelength of the Rayleigh waves is about 8 m, which is equal to the depth of the tunnel. This ensures the amplitude of the Rayleigh-wave diffraction can be as strong as possible due to the energy distribution in different frequencies.

The tunnels are supposed to be filled with air. Hence the P-wave velocity inside the tunnel is the acoustic wave velocity (342 m/s). The S-wave velocity is zero. The density is the air density under a standard temperature and pressure (1.27 kg/m^3). A problem for modeling surface-waves with air-earth boundary is how to make appropriate free-surface conditions (e.g. Xu et al., 2007). For simplicity, we use the conventional vacuum-elastic free surface condition, which means no air coupled waves will be simulated in the synthetic records.

For modeling algorithm, we use the standard Virieux (1986) staggered-grid 4^{th} order finite-difference scheme with perfectly matched layer (PML) absorbing boundaries. Each model has the exact same modeling parameters except the tunnel size. The grid size is 0.125 m × 0.125 m. Time step size for modeling is set to 0.01 ms to avoid numerical dispersion. Figure 1 shows the synthetic seismograms of tunnel sizes of 4 m × 4 m, 2 m × 2 m, 1 m × 1 m and 0.5 m × 0.5 m.

Figure 2 shows the normalized single trace record (vertical particle velocities) of different models. As anticipated, the amplitude of Rayleigh-wave diffraction decreases with reducing the size of the tunnel. Through equation (1), we can calculate the arrival time of diffracted Rayleigh waves. By picking the peak value of Rayleigh-wave diffraction amplitude for different models, we can generate a curve that represents the amplitude variation versus the size/depth ratio of a tunnel.

Modeling Results and Conclusions

Figure 3 shows a curve of the relationship between the energy of Rayleigh-wave diffraction and the size/depth ratio of a tunnel. The horizontal axis is the ratio of size/depth of a tunnel. The vertical axis is the absolute value of the amplitude of Rayleigh-wave diffraction. For the convenience of calculation, the amplitude values are normalized from 0 to 100. Since direct Rayleigh waves always dominate the energy distribution of the 2-D P-SV wavefield, the normalized amplitude values of the seismic waves on the record are also the percentage of their energy compare to the direct Rayleigh waves.

By analysis on the amplitude of a single trace record, we found that the energy of P-waves is about 10% of that of Rayleigh waves. Because no noise was introduced during the modeling process, we can always get the diffraction hyperbola by simply increasing the gain of synthetic record. However, for real data, it is not always possible due to the existence of noise. Here we will consider that if the diffraction energy is less than 10% of the body waves, i.e. 1% of the original Rayleigh waves, then it will be impractical to recognize the diffraction pattern on a real shotgather.

Through Figure 3 we can see clearly that the Rayleigh-wave diffraction energy decreases moderately when the tunnel size is greater than about 3/16 of the central depth of a tunnel. However, if the tunnel size is smaller than 3/16 of its depth, reducing the tunnel size leads to a more rapid decrease of Rayleigh-wave diffraction energy. When a tunnel size is smaller than 1/32 of its depth, the diffraction energy of Rayleigh-wave is less than 1% of the direct Rayleigh-wave energy. In this case, the diffraction energy is considered too weak to be separated from the background noise for real-world application.

Finally, it should be noted that the above results are based on numerical modeling, which is an entirely noise free process. However, the real data always contains noise, which makes the recognition of Rayleigh-wave diffraction more challenging. No explicit attenuation of energy is accounted during the modeling. Since attenuation in the real world is more complicated (e.g., the near-surface attenuation), the energy of Rayleigh-wave diffraction can be much weaker than the modeling results. Hence, for real data, the ratio of size to depth of a detectable tunnel could be much larger than these modeling based results.

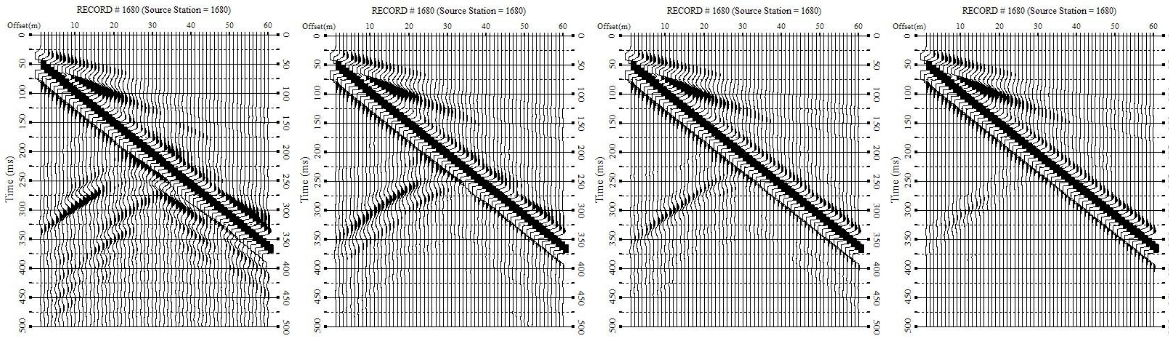

(a) (b) (c) (d)

Figure 1: Synthetic seismograms generated from different models. All the shotgathers use the same ploting parameters (gain, etc.). The central depth of tunnels is 8 m with a size of: (a) 4 m × 4 m (b) 2 m × 2 m (c) 1 m × 1 m (d) 0.5 m × 0.5 m.

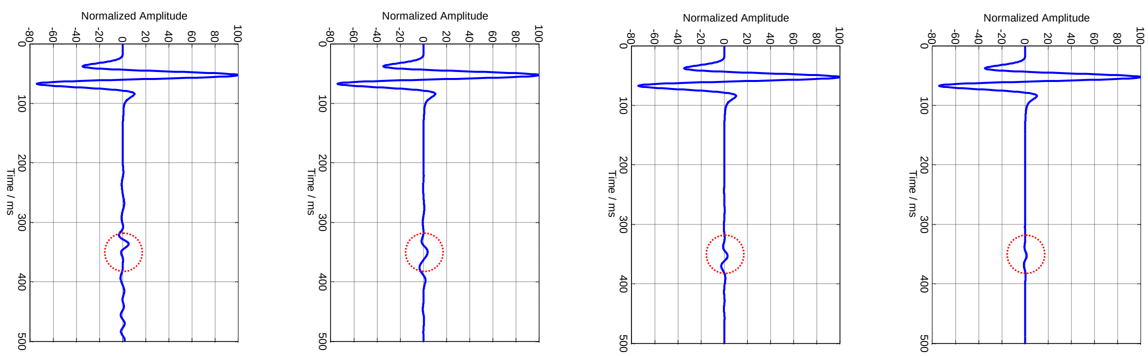

(a) (b) (c) (d)

Figure2: Normalized single trace record of different models. The amplitude of Rayleigh-wave diffraction are marked on the curves. The central depth of tunnels is 8 m with a size of: (a) 4 m × 4 m (b) 2 m × 2 m (c) 1 m × 1 m (d) 0.5 m × 0.5 m.

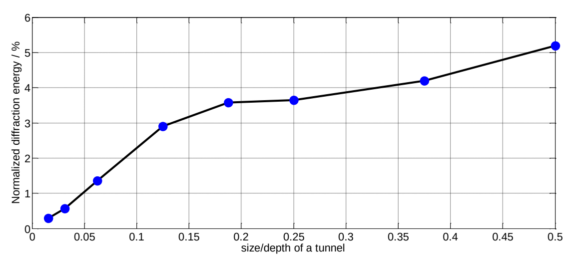

Figure 3: Relationship between the Rayleigh-wave diffraction energy and the size/depth ratio of the tunnel.

EDITED REFERENCES

Note: This reference list is a copy-edited version of the reference list submitted by the author. Reference lists for the 2009 SEG Technical Program Expanded Abstracts have been copy edited so that references provided with the online metadata for each paper will achieve a high degree of linking to cited sources that appear on the Web.

REFERENCES

Campman, X. H, K. van Wijk, C. D. Riyanti, J. Scales, and G. C. Herman, 2004, Imaging scattered seismic surface waves: Near Surface Geophysics, **2**, 223–230.

Gelis, C., D. Leparoux, J. Virieux, A. Bitri, S. Operto, and G. Grandjean, 2005, Numerical modeling of surface waves over shallow cavities: Journal of Environmental and Engineering Geophysics, **10**, 111–121.

Miller, R. D., J. Xia, C. B. Park, and J. Ivanov, 1999, Multichannel analysis of surface waves to map bedrock: The Leading Edge, **18**, 1392–1396.

Song, Y. Y., J. P. Castagna, R. A. Black, and R. W. Knapp, 1989, Sensitivity of near-surface shear-wave velocity determination from Rayleigh and Love waves: 59th Annual International Meeting, SEG, Expanded Abstracts, 509–512.

Virieux, J., 1986, P-SV wave propagation in heterogeneous media: Velocity-stress finite-difference method: Geophysics, **51**, 889–901.

Xia, J., R. D. Miller, and C. B. Park, 1999, Estimation of near-surface shear-wave velocity by inversion of Rayleigh wave: Geophysics, **64**, 691–700.

Xia, J., R. D. Miller, C. B. Park, J. A. Hunter, J. B. Harris, and J. Ivanov, 2002, Comparing shear-wave velocity profiles from multichannel analysis of surface wave with borehole measurements: Soil Dynamics and Earthquake Engineering, **22**, 181–190.

Xia, J., C. Chen, P. H. Li, and M. J. Lewis, 2004, Delineation of a collapse feature in a noisy environment using a multichannel surface wave technique: Geotechnique, **54**, 17–27.

Xia, J., C. Chen, G. Tian, R. D. Miller, and J. Ivanov, 2005, Resolution of high-frequency Rayleigh wave data: Journal of Environmental and Engineering Geophysics, special issue on seismic surface waves, **10**, 99–110.

Xia, J. Y. Xu, R. D. Miller, and C. Chen, 2006, Estimation of elastic moduli in a compressible Gibson half-space by inverting Rayleigh-wave phase velocity: Surveys in Geophysics, **27**, 1–17.

Xia, J., J. E. Nyquist, Y. Xu, M. J. S. Roth, and R. D. Miller, 2007, Feasibility of detecting near-surface feature with Rayleigh-wave diffraction: Journal of Applied Geophysics, **62**, 244–253.

Xu, Y., J. Xia, and R. D. Miller, 2007, Numerical investigation of implementation of air-earth boundary by acoustic-elastic boundary approach: Geophysics, **72**, SM147–SM153.